Effect of Copper Loading in Copper-Alumina Aerogels on Three-Way Catalytic Performance

Ann M. Anderson, Braford A. Bruno, Frank Dilone, Matthew T. LaRosa, Thomas F. Andre, Chris Avanessian & Mary K. Carroll

Emission Control Science and Technology

ISSN 2199-3629

Emiss. Control Sci. Technol.
DOI 10.1007/s40825-020-00165-z

Springer

Emission Control Science and Technology
https://doi.org/10.1007/s40825-020-00165-z

SPECIAL ISSUE: 2019 CLEERS OCTOBER 17 - 19, ANN ARBOR, MI, USA

Effect of Copper Loading in Copper-Alumina Aerogels on Three-Way Catalytic Performance

Ann M. Anderson[1] · Braford A. Bruno[1] · Frank Dilone[1] · Matthew T. LaRosa[1] · Thomas F. Andre[2] · Chris Avanessian[2] · Mary K. Carroll[2]

Received: 15 December 2019 / Revised: 10 May 2020 / Accepted: 6 June 2020

Abstract

Aerogels are high surface area, low density, low thermal mass, nanoporous materials that are stable at high temperatures. This unique combination of physical characteristics makes them promising for use in three-way catalyst systems. Their high surface area has the potential to result in more active sites and improved gas/solid interaction. Their high temperature stability may reduce active site diffusion/sintering and allow for close coupling, which combined with the low thermal inertia may lead to a reduced time to light-off. It is relatively easy to incorporate a variety of metals, including non-precious group metals, into an aerogel backbone. We have developed a series of copper-alumina (CuAl) aerogels via sol-gel synthesis and rapid supercritical extraction drying. Different amounts of copper were incorporated into the alumina gel, resulting in materials with 20% to 40% copper by mass. Scanning electron microscopy imaging shows copper-containing particles distributed in the material, and powder X-ray diffraction indicates that the copper may be in the copper aluminate spinel phase after heat treatment. The materials were tested in the Union Catalytic Aerogel Testbed (UCAT), which evaluates catalytic material performance for conversion of NO, HCs, and CO over a range of temperatures from 200 to 700 °C using a simulated exhaust gas mixture with and without air. UCAT test results indicate that adding more copper to the aerogel lowers the light-off temperature from 350 to 225–250 °C for the conversion of CO and from 500 to 425–450 °C for the conversion of HCs (in the presence of air) and from 425 to 325 °C for NO (without air).

Keywords Catalyst · Three-way catalyst · Copper-alumina aerogel

1 Introduction

Exhaust from automobiles and light trucks is a significant source of air pollution. Regulatory demands on emissions, new engine cycles, and new fuels change the operating characteristics faced by after-treatment systems and create technical challenges for exhaust mitigation. The major pollutants of concern associated with modern automotive gasoline engines are carbon monoxide (CO), various oxides of nitrogen (NO, NO_2) collectively referred to as NOx, and a myriad of unburned hydrocarbon species, typically in vapor form, collectively referred to as HCs. The current industry-standard after-treatment solution for gasoline engines, the "catalytic converter" or three-way catalyst (TWC), oxidizes the HCs to CO_2 and H_2O, oxidizes the CO to CO_2, and reduces the various NOx species to N_2 and O_2. To achieve acceptable performance, modern TWCs use some combination of platinum, palladium, and rhodium, often in combination with an oxygen storage component such as ceria, washcoated with a slurry of alumina onto a ceramic honeycomb substrate. Formulations and configurations are designed and continually modified to meet changing regulatory mandates, performance, and cost goals.

Challenges faced by TWC technology include the high cost, high environmental impact (due to mining), and uncertain supply (influenced by geopolitics) of the platinum group metals (PGMs) used in TWCs. Thus, there is substantial emphasis on research aimed at minimizing the quantity of the PGMs used in automotive catalysts [1, 2], as well as maximizing the activity, minimizing the light-off temperature [3], and

---

✉ Ann M. Anderson
andersoa@union.edu

[1] Department of Mechanical Engineering, Union College, Schenectady, NY 12308, USA

[2] Department of Chemistry, Union College, Schenectady, NY 12308, USA

increasing the longevity [3–5] of the PGMs that are used. Catalytic materials with high surface area and number of active sites but minimal thermally induced aging are sought.

Another key issue in TWC technology is the need to reduce HC emissions associated with the "cold start." Between 60 and 80% of all HC emissions is typically emitted during the first 2 min of the US Federal Test Protocol, before the catalyst has begun to operate efficiently [6]. To meet low-emission vehicle or ultra-low-emission standards, the catalyst light-off temperature must be reduced, the time required to reach the light-off temperature (i.e., temperature for 50% conversion) must be reduced, or both. Stability at elevated operating temperature is also desirable as this facilitates positioning the TWC closer to the exhaust ports so initial heating to the light-off temperature will be as rapid as possible. Novel catalyst materials and substrates with low thermal inertia and low thermal conductivity offer significant potential benefits for reaching light-off temperature rapidly.

Aerogels are materials with a unique combination of properties including low density, low thermal mass, high surface area, and excellent thermal stability. This unique combination of physical characteristics makes them promising for use in three-way catalysis systems. Their high surface area has the potential to result in more active sites and improved gas/solid interaction. Their high temperature stability may reduce active site diffusion (sintering) and allow for close coupling, which combined with the low thermal inertia may lead to a reduced time to light-off. The aerogel structure consists of nanoscale-sized spherical clusters linked together in chains, ultimately forming an amorphous spatial grid with air-filled pores on the order of tens of nanometers. Aerogels can be readily tailored for catalytic activity by combining a catalytically active metal species within the aerogel support matrix (see, for example, review articles by Pajonk [7–10] and Choi [11]).

Aerogels can be synthesized using metal alkoxides [7, 10] or inorganic salts [12] as precursors; the specific source determines the composition of the resulting matrix. Metal oxide aerogels can catalyze reactions without the use of noble metals, and they are more thermally stable than bulk metal oxide transition phases. Silica-based aerogels have excellent thermal stability, and alumina-based aerogels have been shown to delay the phase transition between γ-alumina (high surface area) and α-alumina (low surface area) to higher temperatures than observed for bulk γ-alumina [13–15]. This stability should help catalytic aerogels maintain good activity after repeated exposure to high temperatures, allowing them to be placed closer to the engine for improved light-off performance, and making them more resilient to thermal degradation. The use of catalytically active aerogels in a TWC could be an attractive alternative to the existing technology because they can address myriad challenges: requirements for high activity and selectivity, minimizing PGM content, maximizing surface area and access to catalytically active sites, minimizing thermal inertia, and maximizing thermal stability.

We have developed a rapid supercritical extraction (RSCE) method for making aerogels [16–18]. Using the RSCE technique, we have succeeded in making catalytically active alumina, titania, titania-silica, silica, and a variety of transition-metal-containing aerogels [19–28]. The bulk physical properties of these aerogels and their structures are comparable to those of aerogels made using conventional techniques. Of these materials, copper-alumina (CuAl) aerogels have shown the best three-way catalytic activity [25, 26].

The purpose of the work presented here is to examine the effect of copper loading on the three-way catalytic performance of copper-alumina aerogels. To do so, we fabricated CuAl aerogels via an impregnation and a co-precursor method with varying amounts of copper and then characterized their physical properties and catalytic performance.

2 Methods and Materials

2.1 Materials

Aluminum chloride hexahydrate, $AlCl_3•6H_2O$ (99%), copper (II) nitrate trihydrate Cu $(NO_3)_2•3H_2O$ (99%), and propylene oxide (> 99%) were acquired from Sigma Aldrich. Reagent-grade and absolute ethanol were acquired from Fisher Scientific. All reagents and solvents were used without additional purification.

2.2 Wet Gel Preparation

The copper-alumina wet gels were prepared using two methods: impregnation [17, 26] and co-precursor [28]. Multiple samples were prepared with some samples used for the copper content studies, while others were used for catalytic and characterization studies.

For the impregnation method (IMP), alumina wet gel was synthesized. First, 5.92 g of aluminum chloride hexahydrate was added to 40 mL of reagent-grade ethanol. After the salt was completely dissolved (~ 20 min), 8.5 mL of propylene oxide was added and gel formation occurred in 4–7 min. The beaker containing the gel was sealed with plastic paraffin film and allowed to age under ambient conditions in a fume hood. After 24 h, excess solvent was poured off and copper was introduced to the wet gel by soaking the alumina gel in a solution containing 2, 4, or 8 g of copper nitrate trihydrate in 40 mL absolute ethanol for 24 h. Two additional solvent exchanges with absolute ethanol were then performed at 24-h intervals to remove excess propylene oxide and other reagents and any byproducts. After each solvent exchange, the volume of solvent poured off the wet gel was measured, and a sample was retained for later testing.

For the co-precursor method (CoP), copper-alumina wet gels were made by dissolving 4 g of copper (II) nitrate trihydrate into a solution containing 5.92 g aluminum chloride hexahydrate in 40 mL reagent-grade ethanol. Then, 8.5 mL of propylene oxide was added. Gel formation took up to 20 min and the subsequent wet gel was allowed to cure under ambient conditions in a beaker sealed with plastic paraffin film for 1 day. Over the course of 3 days, solvent exchanges with 40 mL absolute ethanol were performed at 24-h intervals to remove excess reagents and byproducts. After each solvent exchange, the volume of solvent poured off the wet gel was measured, and a sample was retained for later testing.

2.3 Aerogel Synthesis

After completion of the solvent exchanges, aerogels were formed from the wet gels using a rapid supercritical extraction (RSCE) method [16–18]. The wet gels were placed into the wells (3.8 cm diameter, 1.5 cm deep) of a 12.7 cm × 12.7 cm × 1.8 cm stainless steel mold, and the wells were topped off with absolute ethanol. The mold was placed between the platens of a Tetrahedron 24-ton MTP-14 hydraulic hot press and covered with a two-part gasket system consisting of a layer of 0.0005-in-thick 302 stainless steel foil (Brown Metals, 302/304FH0005) and 0.0625-in-thick flexible graphite sheet (Phelps, 7500). The mold was then sealed using a 200-N load and heated to a supercritical state of 249 °C at a rate of 3.8 °C/min with a constant load of 200 N. Upon reaching 249 °C, the system dwelled for 30 min to allow the system to equilibrate. The press force was then decreased to 4.4 N at a rate of 4.4 N/min which allowed supercritical fluid to escape from the mold. After a 15-min dwell, the mold was then cooled to 32 °C at a rate of 3.8 °C/min. The entire RSCE process took approximately 4 h.

2.4 Heat Treatment

All aerogel samples were calcined before catalytic testing. The aerogels were put into loosely covered Pyrex crucibles, which were then placed in a Thermo-Scientific Thermolyne furnace for heat treatment at 800 °C for 24 h.

2.5 Slurry Studies

After catalytic testing, samples were slurried by adding 4 mL of aerogel to 20 mL of deionized water. The mixture was stirred using a magnetic stirrer for 1.5–3.5 h, and then placed on a hot plate and heated to 60–65 °C to dry (24–48 h).

2.6 Determination of Copper Loading

The amount of copper in the gels was calculated indirectly, by employing an Agilent 8453 UV-Visible diode-array spectrophotometer to determine the amount of copper that remained in the solvent following each solvent exchange (and, therefore, was not incorporated into the gel). The volume of liquid poured off the wet gel in each step was measured, and then the concentration of copper (II) in the extract was determined. The total amount of copper (II) lost during the solvent exchanges was then subtracted from the initial amount of copper (II) in the salt. This approach assumes that the only loss of copper occurs during the solvent exchanges and, therefore, the value determined represents an upper bound of the amount of copper in the aerogel.

For gels prepared via impregnation, an external calibration curve could be employed because the visible absorption spectra of the exchange solutions matched that of a standard solution of copper (II) nitrate trihydrate in absolute ethanol. The absorbance of each of a series of nine standard solutions (0.0033 to 0.090 M Cu^{2+} in absolute ethanol) was recorded at 760, 800 (λ_{max}) and 840 nm, and linear Beer-Lambert Law plots were prepared [29]. After each exchange, the total volume of solvent poured off the wet gel and the absorbance of an aliquot of this solution were measured. The calibration curve was then used to determine the concentration of copper (II) in the solvent removed during each exchange. The total amount of copper (II) in the exchange solution was calculated from the concentration and the volume.

Due to matrix effects, a standard addition method [29] was employed for quantitation of copper in the co-precursor gels. The copper (II)-containing liquid mixture poured off the wet gel was a visibly different color (and therefore had a different absorption spectrum) than the copper (II) chloride in ethanol standard solutions. After each exchange, a 2100-μL sample of the extracted solvent was pipetted into a cuvette, and its absorbance at 760, 800, and 840 nm was recorded. Then a series of small-volume aliquots of a stock solution of copper (II) in absolute ethanol was added to the cuvette with absorbance recorded again after each "spike." Ideally, the first "spike" would double the absorbance of the sample; each subsequent aliquot was of the same volume as the first. A plot of absorbance (at 760, 800, and 840 nm) vs. concentration of added Cu^{2+} was prepared. The absolute value of the x-intercept of the line yields the concentration of copper (II) in the extract liquid, and the total amount of copper (II) in the exchange solution was calculated from this concentration and the volume.

3 Characterization Methods

3.1 Scanning Electron Microscopy

Scanning electron micrographs (SEM) were acquired with a Zeiss EVO MA15, and energy dispersive X-ray (EDX) spectra and maps were acquired using a Horiba Scientific iHR 320 with a Bruker XFlash 6130 detector. During operation of the EDX, the electron gun was set to a beam voltage of 12 kV and a spot size of 500 Å, the working distance was adjusted to 8 mm, and data was collected for approximately 3 min using the "enhanced" color mixing option. Samples were prepared by lightly grinding the aerogel pieces with a mortar and pestle and attaching them to mounts using carbon tape. The samples were imaged without further treatment.

3.2 Gas Adsorption

A Micromeritics ASAP 2020 Gas Adsorption system was used to measure the surface area and pore distribution of the CuAl aerogels. Samples were gently crushed using a mortar and pestle. Approximately 0.2 g of sample was placed in a sample tube and degassed by heating to 90 °C for 2 h and then 200 °C for 6 h. After degassing, the sample was analyzed using the ASAP 2020 with a 20-s equilibration time for relative partial pressures below 0.9 and a 35-s equilibration time for relative partial pressures above 0.9. Longer equilibration times were used at high partial pressures to avoid the effects of compression at high pressure [30]. BET surface area was determined using five points at relative partial pressures from 0 to 0.30. BJH pore distributions were evaluated using the desorption isotherms.

3.3 Powder X-Ray Diffraction

Powder XRD patterns were acquired using a Phillips PW-1840 X-ray diffractometer equipped with a copper X-ray source tube with a nickel filter. Each sample was crushed into a powder and packed into an open-backed aluminum sample holder. Diffraction patterns were taken over a 2θ range of 2°–80° using a tube voltage of 45 keV and a 40-mA current. Diffraction patterns were analyzed using Rigaku SmartLab Studio II Software with the ICDD PDF-2 database.

3.4 Catalytic Testing

The Union Catalytic Aerogel Testbed (UCAT), shown schematically in Fig. 1 and described more fully in Bruno et al. [25], was used to measure the catalytic ability of the aerogels. Small samples of aerogel (ca. 20 mL) were placed in one of two identical packed bed test sections, which in turn were placed in a furnace (ThermCraft 9800W Split Tube) controlled by the UCAT system to maintain the samples at the desired temperature set point during a test. The temperature of the reactant gases flowing through the aerogel beds was monitored by thermocouples placed in the inlet and outlet flows of the packed beds.

A gas mixing system (not shown) was used to mix and bottle custom exhaust simulant blends including hydrocarbons, nitrogen oxides, and carbon monoxide. The resulting gas bottle (labeled "gas mix" on the schematic, Fig. 1) was then connected to the UCAT system, which metered the flow of gas through the test sections. Oxygen was not added at the bottling stage (to maintain storability of the blends); instead, when desired, oxygen was added by the flow control system via air addition to the test section flow stream. For the tests performed in this study, we used an exhaust simulant blend based on California BAR 97 LOW emissions 32 blend calibration gas (300 ppm NO, 0.5% CO, 6.0% CO_2, 200 ppm propane (i.e., HC), in a balance of N_2). The blend was used "neat" (no air addition) as a crude simulation of "fuel rich" combustion products. "Fuel lean" (i.e., excess oxygen) combustion products were simulated by adding a small flow of air to the bottled mixture, resulting in final concentrations of 0.36% O_2, 295 ppm NO, 0.49% CO, 5.9% CO_2, 197 ppm propane, in a balance of N_2. These two conditions are referred to simply as "No Air" and "Air" in the results below.

For all results presented here, UCAT was set to maintain a constant 72,000 h^{-1} space velocity, based on the aerogel sample volume used, regardless of the test temperature or "Air"/"No Air" condition being examined. As described above, the as-prepared aerogels were heat treated at 800 °C prior to testing, and 20 mL of crushed aerogel monolith was used in the packed bed reactor test section for each test. Pollutant conversion efficiency tests were conducted over a range of steady state temperatures from 200 to 600 °C at approximately 50 °C intervals. The temperature reported was the average of the inlet and outlet gas flow temperatures.

At each test condition, concentrations of CO, NO, and HC (pollutant concentrations) as well as CO_2 and O_2 were measured with commercial five-gas analyzers (Infrared Industries FGA4000XDS 5 Gas Analyzer, one per test cell). Untreated gas concentrations (obtained via the bypass lines) were measured immediately prior to and immediately after each treated gas concentration measurement to monitor and correct for any instrument drift. The conversion efficiency was calculated from these measurements. Two test sections were used to increase testing throughput.

4 Results and Discussion

4.1 Aerogel Appearance

Copper-alumina wet gels are aqua green in color (not shown). As-prepared IMP CuAl aerogels are red in color

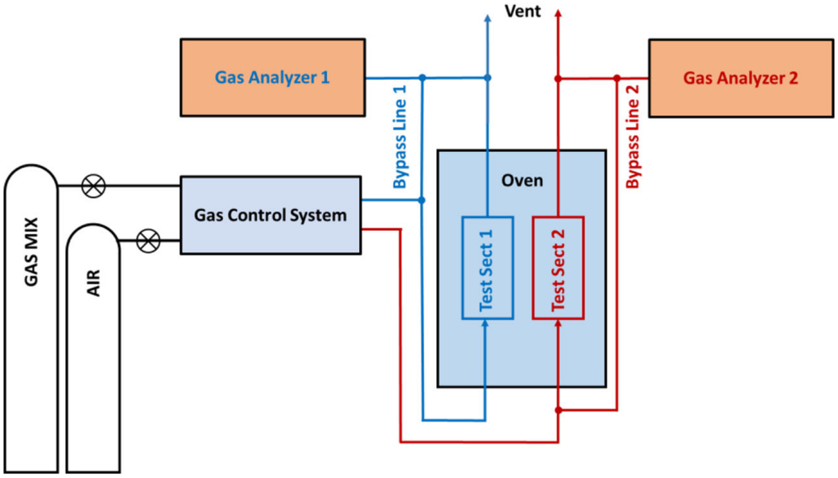

Fig. 1 Schematic of UCAT system. The gas mixture and air are metered through the gas control system and into the oven, which contains two test sections containing the samples to be tested. A five-gas analyzer was used to measure the input concentrations through the bypass line and the output concentrations at the oven exit

(4-IMP shown in Fig. 2a) and turn a deep red (Fig. 2b) following heat treatment at 800 °C in air for 24 h. Intermediate color changes were observed upon heat treatment to lower temperatures and/or for shorter periods of time [26]. In an related study, RSCE cobalt-alumina aerogels withstood heat treatment to temperatures as high as 1100 °C [15].) The as-prepared 4-CoP aerogel pieces have a green exterior with red interior (Fig. 2c); they are uniformly red in color following heat treatment in air to 800 °C for 24 h (Fig. 2d). Additional color changes were not observed after catalytic testing. The aerogels shrunk considerably during calcination (67% decrease in volume and 33% decrease in mass for the 4-IMP aerogels, and 73% in volume and 49% in mass for the 4-CoP aerogels) presumably due to densification via thermal sintering and removal of any solvent adsorbed on the as-prepared aerogels.

4.2 Copper Content

Copper-alumina aerogels were made using either 2, 4, or 8 g of copper (II) nitrate trihydrate (0.53, 1.05, and 2.1 g of copper, respectively) via the impregnation method, or using 4 g of the salt in the co-precursor method. Table 1 presents the results for the amount of copper retained in the wet gels and Table 2 presents that for the aerogels.

The amount of copper in the impregnation samples is dependent on how much copper adheres to the wet alumina gel during the first solvent exchange as well as any loss in subsequent exchanges. Based on analysis of the solvent from the first exchange (which is the impregnation step), there was 94% uptake of copper for the 2-IMP aerogels, 80% uptake for the 4-IMP aerogels, and 65% uptake for the 8-IMP aerogels; however, some copper likely remained in solution phase within the pores of the gel, rather than being incorporated into the solid matrix. Some of the copper then diffused and/or was leached out during subsequent exchanges (3, 11, and 22% in the second exchange and an additional 2, 6, and 7% in the third exchange for the 2-, 4-, and 8-IMP gels respectively). In the synthesis of the co-precursor samples, copper was incorporated into the gel matrix during the gelation process (yielding 100% uptake); some diffusion and/or leaching of the copper was observed during the subsequent solvent exchanges. For the 4-CoP samples, a total of ca. 3% of the copper leached out yielding retention of 97% of the copper.

After RSCE processing, the copper mass content per gram of aerogel was estimated using the solvent analysis results of copper content and mass measurement of each aerogel sample. Results are presented in Table 2 and indicate that for the as-prepared IMP samples, copper content by mass increased as copper (II) salt was added to the alumina wet gel (ranging

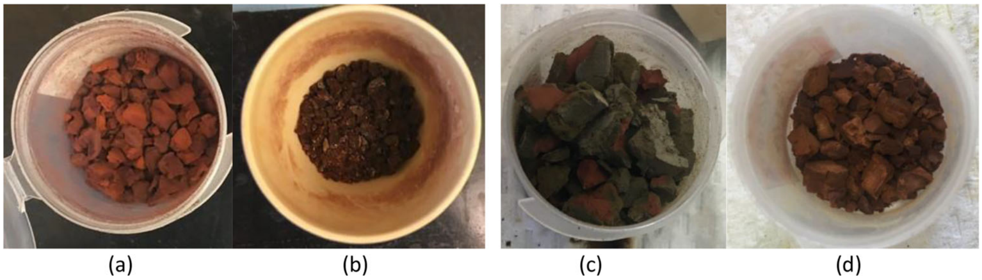
(a) (b) (c) (d)

Fig. 2 Photographs of CuAl aerogels: 4-IMP **a** as prepared and **b** post heat treatment; 4-CoP **c** as prepared and **d** post heat treatment

Table 1 Copper content analysis of wet gel samples

Sample type	Copper added from salt (g)	Copper in remaining wet gel (g)	% Loss of Cu in wet gel
2-IMP	0.537 ± 0.009 (3)	0.48 ± 0.04 (3)	10 ± 7
4-IMP	1.063 ± 0.009 (18)	0.71 ± 0.08 (18)	33 ± 8
8-IMP	2.119 ± 0.003 (3)	$1.0 \pm 0.2_5$ (3)[a]	50 ± 10
4-CoP	1.065 ± 0.007 (9)	1.03 ± 0.02 (9)	3 ± 2

Data is presented as the average plus or minus one standard deviation with the number of samples analyzed indicated in parentheses

[a] The large relative standard deviation for the 8-IMP aerogels is due to one sample that we suspect is an outlier. Without that sample, the copper remaining is calculated to be 1.12 ± 0.03 (g) with a 47 ± 2% loss)

from 220 to 370 mg/g). The mass ratio of copper in the 4-CoP sample is similar to that of the 4-IMP sample; however, post heat treatment the copper mass ratios differ.

These results indicate that, as expected, the co-precursor method is able to better incorporate and retain copper in the aerogel.

4.3 Surface Area and Pore Distribution

BET surface area results are presented in Table 3 for as-prepared, post heat treatment, post-UCAT, and post-slurry samples. The as-prepared materials have relatively high surface area, which is in agreement with our previous work [26]. After heat treatment, in addition to the mass and volume changes described above, these materials exhibit a significant drop in surface area (likely due to densification via thermal sintering) [26]. Based on our previous work, the surface area does not change further after UCAT testing so we expect that the post-UCAT surface area values for the 2-IMP, 8-IMP, and 4-CoP aerogels presented in Table 3 are similar to post heat treatment results as it is for the 4-IMP aerogel. The results show that there is no further change in surface area after slurrying in water (neutral pH), indicating that it may be possible to washcoat these materials without performance degradation.

The BJH pore distributions (not shown) for the as-prepared materials showed pores in the 10–80 nm range with peak pore volume occurring at about 35 nm. After UCAT testing, the peaks diminished and the distributions showed overall reduced pore volume. After slurrying, small peaks reappeared in the 30–40 nm range for the 4- and 8-IMP samples and in the 20–30 nm range for the 2-IMP sample.

4.4 Powder X-Ray Diffraction

Powder XRD results are plotted in Fig. 3 for heat-treated aerogels prepared via the impregnation method. In previous work [26], we attributed the large peaks observed in heat-treated CuAl aerogel samples (31°, 37°, 45°, 60°, and 66°) to the presence of γ-alumina, based on comparison to the literature. However, the SmartLab Studio II software indicates that the XRD patterns of the 4- and 8-IMP samples more closely match that of the copper aluminate spinel $CuAl_2O_4$ (ICDD PDF-2 card 01-075-4272). The XRD pattern for the 2-IMP sample is identified as a better match to an aluminum oxide (ICDD PDF-2 card 01-076-4179) but also matches the spinel pattern. For comparison, the XRD pattern for an undoped alumina aerogel (converted from Juhl et al. [23] data acquired with a Co-Kα X-ray source) is also plotted and shows broad peaks at 37°, 45°, and 66°, but no evidence of peaks at 31°, 58°, or 60°.

Table 2 Copper content analysis of aerogel samples

	As prepared		Heat treated	
Sample type	Copper content by mass (mg/g)	Density (g/mL)	Copper content by mass (mg/g)	Density (g/mL)
2-IMP	220 ± 20 (3)	0.15 ± .05 (3)	–	–
4-IMP	290 ± 40 (17)	0.12 ± .02 (17)	450 ± 70 (14)	0.24 ± 0.03 (14)
8-IMP	370 ± 10 (3)	0.1293 ± .0001 (3)	–	–
4-CoP	330 ± 10 (8)	0.12 ± .02 (8)	650 ± 50 (8)	0.24 ± 0.02 (8)

Data is presented as the average plus or minus one standard deviation with the number of samples analyzed indicated in parentheses. Density is calculated from the estimated volume and mass of each sample

Table 3 BET surface area results for CuAl aerogel samples

	BET surface area (m^2/g)			
Sample	As prepared	Post HT	Post-UCAT	Post Slurry
2-IMP	330 ± 20	–	160 ± 10	156 ± 9
4-IMP	380 ± 20	76 ± 5	83 ± 5	84 ± 7
8-IMP	250 ± 20	–	75 ± 4	74 ± 4
4-CoP	210 ± 10	–	49 ± 3	56 ± 3

Data is presented as the measured surface area for a single sample plus or minus the uncertainty in that measurement, which includes the effects of the BET fit and sample mass measurement

4.5 SEM/EDX Imaging

SEM backscattered electron and EDX images of all of the as-prepared CuAl aerogels show copper-containing particles. Typical images of 4-IMP aerogels (Fig. 4) show a relatively dense distribution of particles with diameter ~ 250 nm or smaller, as well as some larger crystalline features (Fig. 4a, b), connected to an amorphous structure. In the 8-IMP (Fig. 5a) aerogels and the interior portion of the as-prepared 4-CoP aerogels (not shown), copper-containing particles are also observed at relatively high density; however, for the 2-IMP samples (Fig. 5b), the particles are not uniformly distributed, and some aerogel pieces have no observable particles (appear fully amorphous).

EDX images of 4-IMP as-prepared aerogels (Fig. 4c) show copper-containing particles (200–1000 nm) on an alumina structure. The lack of oxygen signal from the particles suggests that they are in the copper(0) form (metallic copper). Similar results were obtained for the other types of aerogels. This is consistent with earlier work: when copper(0), copper(I), or copper (II) containing nanoparticles were incorporated into silica aerogels prepared via rapid supercritical extraction, copper(0) nanoparticles were observed in all of the resulting materials [27]. In addition, the 2-IMP and exterior portions of 4-CoP aerogels show microcrystals with different shape in which copper and chlorine appear to be co-located, suggesting chloride salts.

Following heat-treatment and catalytic testing, the materials contain a relatively even distribution of particles (Fig. 6), with diameter ~ 200 nm or smaller, on an overall amorphous aerogel backbone. There is no evidence of agglomeration. The EDX images (Fig. 6b–d) show clearly that the particles contain copper, with relatively even distribution of aluminum and oxygen atoms throughout the materials.

4.6 Catalytic Performance

Figure 7 plots the catalytic test results for conversion of CO and HC with air in the simulated exhaust mixture and NO without air in the simulated exhaust mixture for the 4-IMP CuAl aerogels; these results represent the base or reference case for CuAl aerogel catalysts. For the other three cases (i.e., CO and HC without air in the simulated exhaust mixture and NO with air), the aerogel catalysts performed no better than an inert sample (data not shown). Three temperature sweeps from 200 to 600 °C were performed on each set of heat-treated samples. Each data point represents a temperature/run condition. Also shown is the conversion for

Fig. 3 X-ray diffraction patterns for the 2-IMP, 4-IMP, and 8-IMP CuAl samples, post heat treatment compared to the pattern for an un-doped alumina aerogel [23]. Traces are offset for clarity

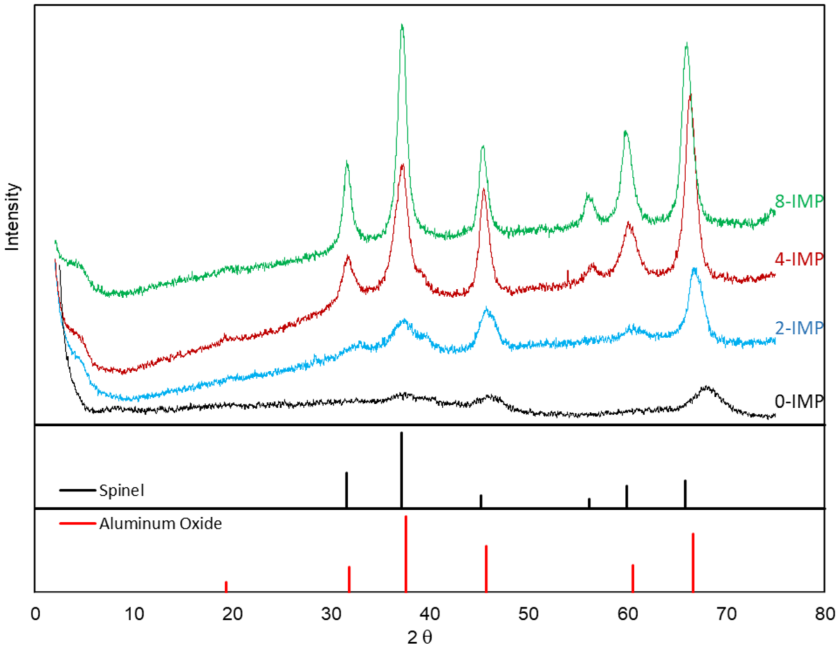

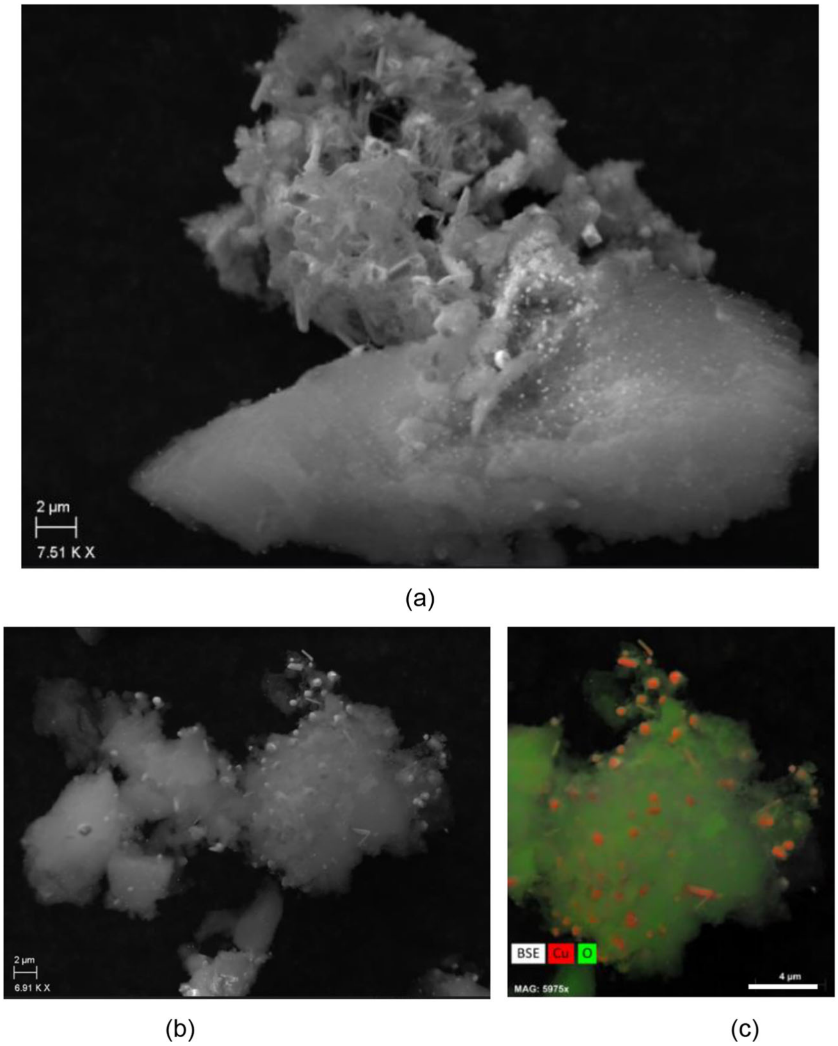

(a)

(b)

(c)

Fig. 4 SEM/EDX images of as-prepared 4-IMP CuAl aerogel: **a** SEM at 7.5 k magnification, **b** SEM at 6.9 k magnification, and **c** EDX at 6.0 k magnification

an inert material (in this case, silica aerogel). The conversion of CO with air reached 100% by 250 °C with light off ~ 225 °C. The HC conversion in the presence of oxygen was modest, not achieving light off until ca. 425 °C. The 4-IMP catalyst showed good activity for NO for the no-air case, lighting off between 300 and 350 °C. In addition, the levels of performance discussed above were stable over time, showing no discernable decrease in performance through at least ten temperature sweeps.

Figure 8 compares the percent conversions for the 2-, 4-, and 8-IMP aerogels for CO, HC, and NO. Only cases for which significant catalytic activity was observed are shown (CO and HC conversion with air, NO conversion without air). In broad terms, there were significant differences in conversion performance between the 2-IMP aerogel on the one hand and the 4- and 8-IMP materials on the other hand. In particular, there was significant improvement in (lowering of) light-off temperature with regard to CO in the presence of oxygen from the 2-IMP (light off ca. 350 °C) to the 4- and 8-IMP (light off ca. 225–250 °C) materials, whereas the difference in light off (if any) between the 4- and 8-IMP was quite small. This pattern of significant difference between the 2-IMP loading vs. similarly performing 4- and 8-IMP samples was repeated in the NO conversion data in the absence of air. Again, we see significant improvement in light off when stepping from the 2-IMP (light off ca. 425 °C) to the others (light off ca. 325 °C), which show essentially indistinguishable performance. All three catalysts were essentially inert to NO in the presence of oxygen over the temperature range studied. The differences in the data for HC conversion in the presence of air showed a weaker but similar trend, with light off decreasing from ca. 500 °C for the 2-IMP to 425 to 450 °C for the 4- and 8-IMP samples. Interestingly, with regard to HCs, the 4- and 8-IMP samples performed very similarly below approximately 400 °C but do possibly diverge above that temperature and follow a trend of performance tracking loading; however, given the small magnitude of the effect and the scatter in the data, this observation should be viewed as tentative.

Figure 9 compares the catalytic ability of the higher performing (4- and 8-IMP) CuAl aerogels made via the

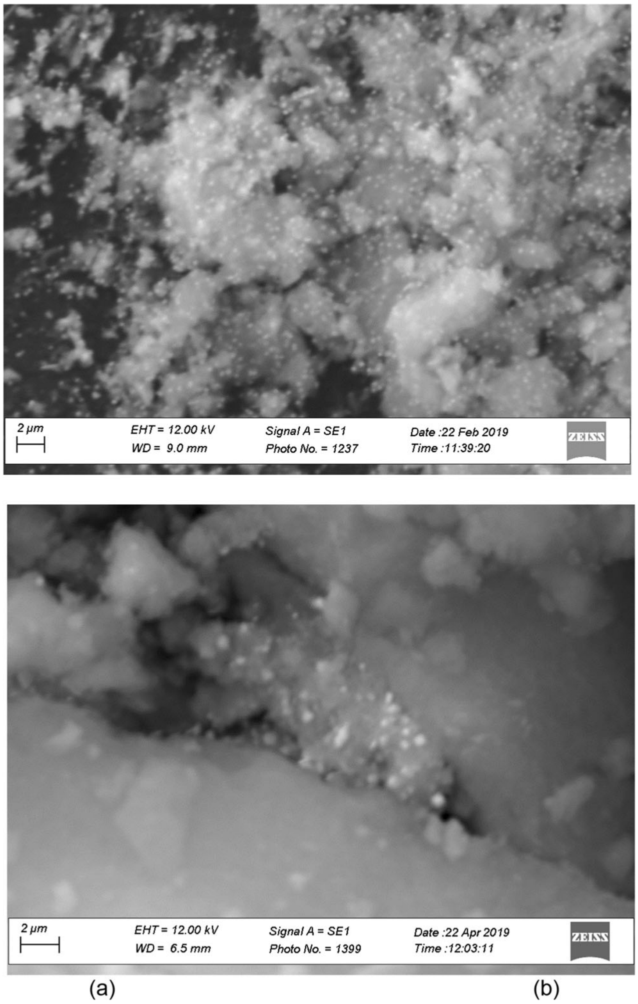

Fig. 5 SEM images of as-prepared **a** 8-IMP CuAl aerogel and **b** 2-IMP CuAl aerogel

impregnation method to the aerogel catalyst made via the co-precursor method (4-CoP). The most significant observation from this comparison is that the co-precursor synthesized catalyst performs very similarly to the two catalysts formed via the impregnation synthesis with higher copper loading (which, as discussed above, perform very similarly to each other).

Finally, it is important to note that, while the above differences and similarities in catalytic performance are discussed in the context of differences in copper loading at synthesis, that should not be taken to imply that it is simply differences in copper abundance that cause the observed performance differences. The SEM and XRD data imply that it is more likely that the formation of more evenly distributed particles of catalytically active copper aluminate spinel is the explanation for at least some of the observed performance differences [31]. Were copper loading in synthesis, in and of itself, the primary factor driving performance, we would expect to see continued improvement from the 4-IMP to the 8-IMP case. However, even the spinel explanation for the performance differences is likely oversimplified. The chemical and physical processes occurring during aerogel processing, heat treating, and catalytic testing are all complex. These can and do change other factors such as the aerogel structure (pore size, tortuosity), distribution and accessibility of active sites, oxidation state of and ligand structure around the copper atoms, each of which has the potential to significantly affect catalytic activity. For example, there are clear differences in the post-testing BET surface areas, with significant decreases between the 2-IMP, the set of 4-IMP and 8-IMP, and the 4-CoP. These differences do not directly correlate with better catalytic performance.

5 Conclusion

We have presented the results of a study on the effect of copper loading at synthesis on the catalytic performance of CuAl aerogels. Increasing the level of copper salt used in synthesis resulted in a significant catalytic performance increase between the lowest concentration studied and the higher ones, with light-off temperatures dropping by approximately 100–125 °C for CO conversion, 50–75 °C for HC conversion, and 100 °C for NO conversion. Further increases in copper retained on a mass basis (in the as-prepared aerogels) did not result in detectible performance enhancement. The step change in performance was accompanied by SEM evidence of increased copper particle formation. We have demonstrated that it is possible to achieve comparable catalytic performance using the impregnation and co-precursor synthetic methods.

In addition to their catalytic performance, these CuAl catalytic aerogels have other properties that demonstrate their promise for eventual application in a TWC. The results of the slurry testing indicate that the materials have the potential to survive a wash-coating process. Moreover, materials showed no evidence of degrading with use: although long-term performance was not a focus of this study, we note that aerogel samples tested for ten or more temperature sweep cycles showed no detectible changes in catalytic ability. Evaluating the structural changes in and the robustness of these materials for long-term performance are areas of ongoing study in our laboratory.

Acknowledgements This material is based upon work supported by the National Science Foundation (NSF) under Grants No. IIP-1918217, IIP-1823899, DMR-1828144 and CBET-1228851. The authors thank Diana E. Lang, Ryan Puglisi, and Christopher O'Brien for assistance with experimental work. MTL and CA are grateful for funding from Union College through the Summer Research Fellowship program. FD acknowledges summer funding from the Union College Mechanical Engineering Department and the Union College Chemistry Department's Kane Fund.

Fig. 6 SEM/EDX images of 4-IMP CuAl aerogel after catalytic testing: **a** SEM at low magnification, **b** EDX image showing copper, **c** EDX image showing oxygen, and **d** EDX image showing aluminum. The scale bar in **b**–**d** is 1 µm

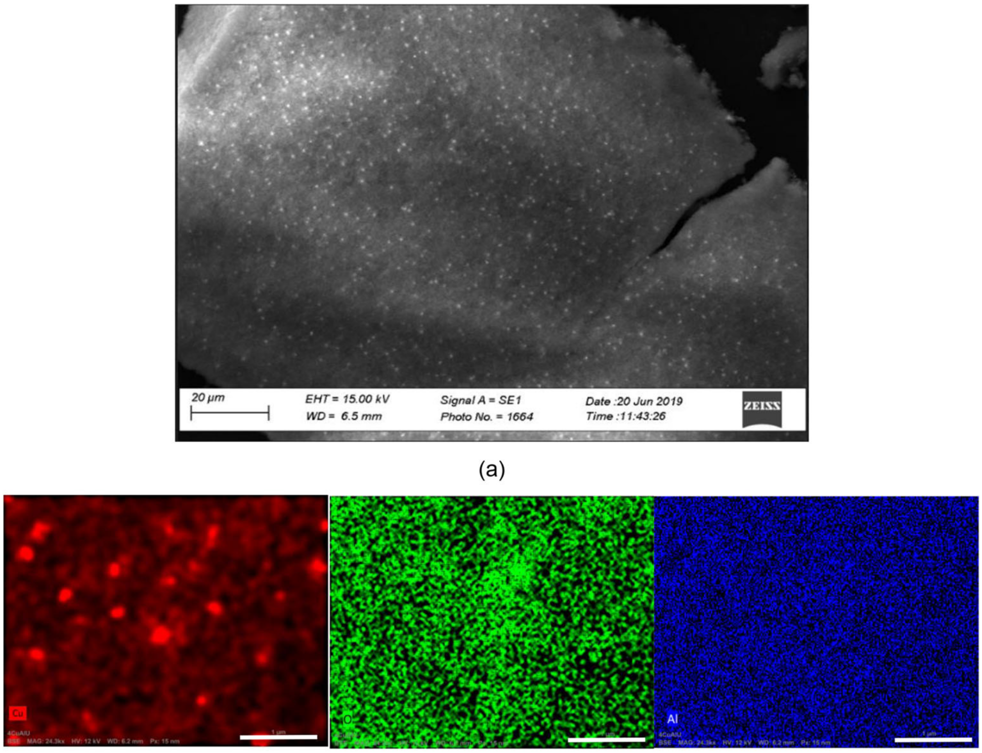

(a)

(b) (c) (d)

Fig. 7 Comparison of the percent conversion of **a** CO and **b** HC, with air in the gas mixture and **c** NO without air in the gas mixture for a 4-IMP CuAl aerogel. Blue circles indicate 4-IMP aerogel; data for inert silica aerogel (green triangles) is provided for comparison. Data from each of three individual tests are plotted for the 4-IMP CuAL aerogel. The average of two runs is plotted for the inert sample

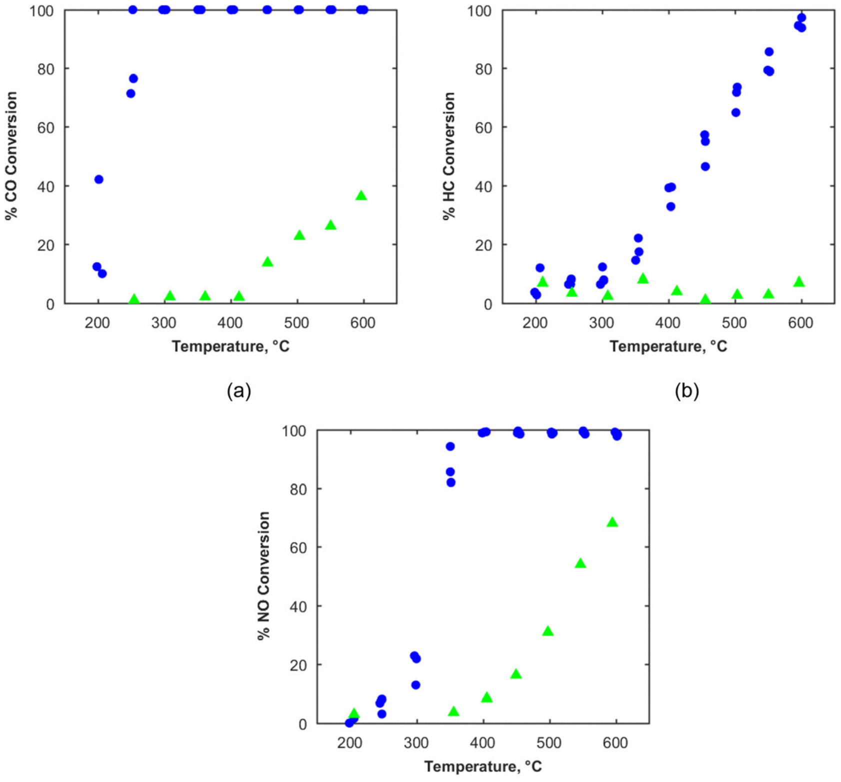

(a) (b)

(c)

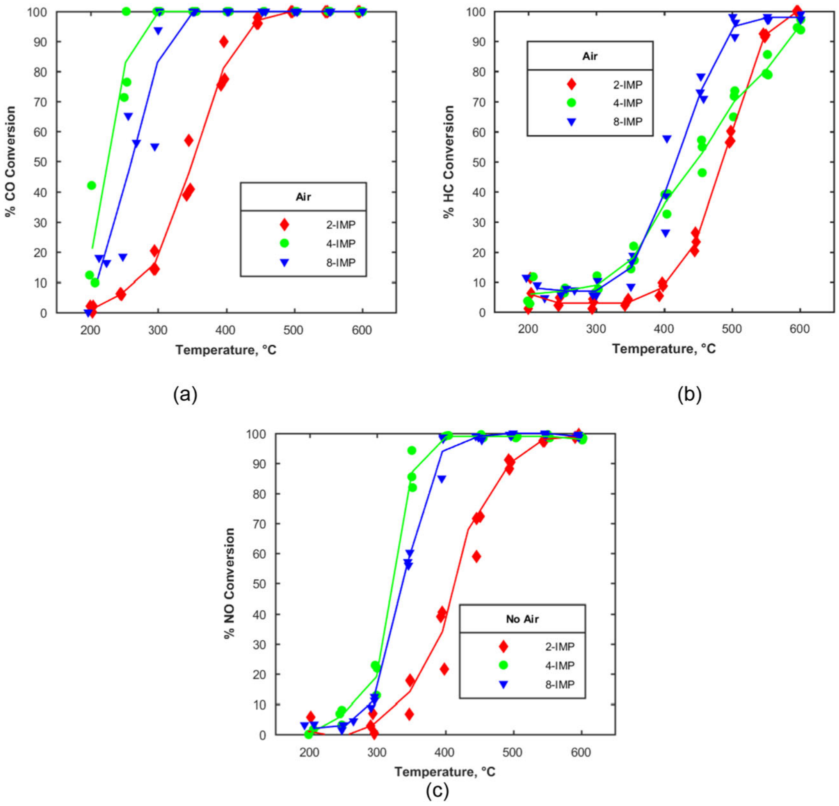

Fig. 8 Comparison of the percent conversion of **a** CO and **b** HC, with air in the gas mixture and **c** NO without air in the gas mixture for or 2-, 4-, and 8-IMP CuAl aerogels. Lines connecting the average performance of each catalyst over three runs at each temperature are included as guides for the eye

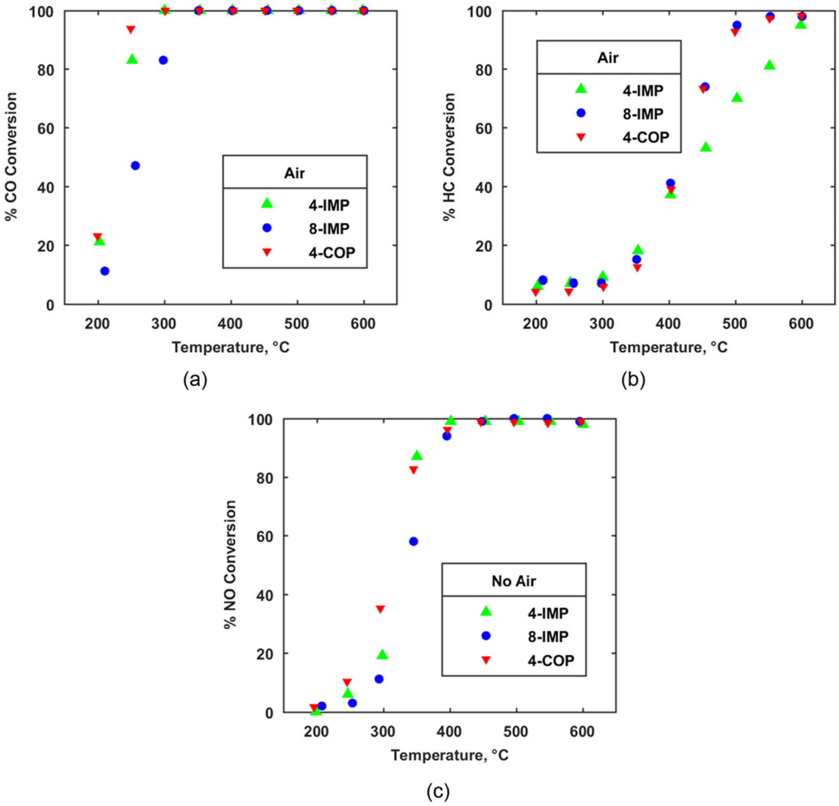

Fig. 9 Comparison of the percent conversion of **a** CO and **b** HC, with air in the gas mixture and **c** NO without air in the gas mixture for 4-IMP, 8-IMP and 4-CoP CuAl aerogels

Compliance with Ethical Standards

Conflict of Interest The authors declare that they have no conflict of interest.

References

1. Johnson, T.V.: SAE 2012 world congress, vehicular emission control highlights of the annual Society of Automotive Engineers (SAE) international congress. Platin. Met. Rev. **57**(2), 117–122 (2013)
2. Cooper, J., Beecham, J.: A study of platinum group metals in three-way autocatalysts. Platin. Met. Rev. **57**(4), 281–288 (2013)
3. Bosteels, D., Searles, R.A.: Exhaust emission catalyst technology. Platin. Met. Rev. **46**(1), 27–36 (2002)
4. He, J.J., Wang, C.X., Zheng, T.T., Zhao, Y.K.: Thermally induced deactivation and the corresponding strategies for improving durability in automotive three-way catalysts. Johnson Matthey Technology Review. **60**(3), 196–203 (2016)
5. González-Marcos, M.P., Pereda-Ayo, B., Aranzabal, A., González-Marcos, J.A., González-Velasco, J.R.: On the effect of reduction and ageing on the TWC activity of $Pd/Ce_{0.68}Zr_{0.32}O_2$ under simulated automotive exhausts. Catal. Today. **180**(1), 88–95 (2012)
6. Heck, R. M., Farrauto, R. J., & Gulati, S. T. (2009). Catalytic Air Pollution Control: Commercial Technology. John Wiley & Sons
7. Pajonk, G.M.: Aerogel catalysts. Appl. Catal. **72**(2), 217–266 (1991)
8. Pajonk, G.M.: Catalytic aerogels. Catal. Today. **35**(3), 319–337 (1997)
9. Pajonk, G.M.: Some catalytic applications of aerogels for environmental purposes. Catal. Today. **52**(1), 3–13 (1999)
10. Pajonk, G.M. (2007). Aerogel synthesis. Ch. 3 in Catalyst Preparation, CRC press
11. Choi, J., Suh, D.J.: Catalytic applications of aerogels. Catal. Surv. Jpn. **11**(3), 123–133 (2007)
12. Gash, A.E., Tillotson, T.M., Satcher Jr., J.H., Hrubesh, L.W., Simpson, R.L.: New sol–gel synthetic route to transition and main-group metal oxide aerogels using inorganic salt precursors. J. Non-Cryst. Solids. **285**(1–3), 22–28 (2001)
13. Keysar, S., Shter, G.E., de Hazan, Y., Cohen, Y., Grader, G.S.: Heat treatment of alumina aerogels. Chem. Mater. **9**(11), 2464–2467 (1997)
14. Horiuchi, T., Osaki, T., Sugiyama, T., Suzuki, K., Mori, T.: Maintenance of large surface area of alumina heated at elevated temperatures above 1300° C by preparing silica-containing pseudoboehmite aerogel. J. Non-Cryst. Solids. **291**(3), 187–198 (2001)
15. Bouck, R.M., Anderson, A.M., Prasad, C., Hagerman, M.E., Carroll, M.K.: Cobalt-alumina sol gels: effects of heat treatment on structure and catalytic ability. J. Non-Cryst. Solids. **453**, 94–102 (2016)
16. Gauthier, B.M., Bakrania, S.D., Anderson, A.M., Carroll, M.K.: A fast supercritical extraction technique for aerogel fabrication. J. Non-Cryst. Solids. **350**, 238–243 (2004)
17. Carroll, M.K., Anderson, A.M., Gorka, C.A.: Preparing silica aerogel monoliths via a rapid supercritical extraction method. JoVE (Journal of Visualized Experiments). **84**, e51421 (2014)
18. Anderson, A.M., Bruno, B.A., Donlon, E.A., Posada, L.F., Carroll, M.K.: Fabrication and testing of catalytic aerogels prepared via rapid supercritical extraction. JoVE (Journal of Visualized Experiments). **138**, e57075 (2018)
19. Bono, M.S., Anderson, A.M., Carroll, M.K.: Alumina aerogels prepared via rapid supercritical extraction. J. Sol-Gel Sci. Technol. **53**(2), 216–226 (2010)
20. Dunn, N.J.H., Carroll, M.K., Anderson, A.M.: Characterization of alumina and nickel-alumina aerogels prepared via rapid supercritical extraction. Polym. Prepr. **52**(1), 250–251 (2011)
21. Brown, L.B., Anderson, A.M., Carroll, M.K.: Fabrication of titania and titania–silica aerogels using rapid supercritical extraction. J. Sol-Gel Sci. Technol. **62**(3), 404–413 (2012)
22. Bruno, B. A., Madero, J. E., Juhl, S. J., Rodriguez, J. Dunn, N. J. H., Carroll, M. K., & Anderson, A. M. (2012). Alumina-based aerogels as three-way catalysts. Proceedings of the 9th Int'l Congress on Catalysis and Automotive Pollution Control (CAPoC9), August 29–31, Brussels, Belgium
23. Juhl, S.J., Dunn, N.J., Carroll, M.K., Anderson, A.M., Bruno, B.A., Madero, J.E., Bono, M.S.: Epoxide-assisted alumina aerogels by rapid supercritical extraction. J. Non-Cryst. Solids. **426**, 141–149 (2015)
24. Smith, L.C., Anderson, A.M., Carroll, M.K.: Preparation of vanadia-containing aerogels by rapid supercritical extraction for applications in catalysis. J. Sol-Gel Sci. Technol. **77**(1), 160–171 (2016)
25. Bruno, B. A., Anderson, A. M., Carroll, M., Swanton, T., Brockmann, P., Palace, T., & Ramphal, I. A. (2016). Benchtop scale testing of aerogel catalysts: preliminary results. SAE Technical Paper No. 2016-01-0920
26. Tobin, Z.M., Posada, L.F., Bechu, A.M., Carroll, M.K., Bouck, R.M., Anderson, A.M., Bruno, B.A.: Preparation and characterization of copper-containing alumina and silica aerogels for catalytic applications. J. Sol-Gel Sci. Technol. **84**(3), 432–445 (2017)
27. Anderson, A.M., Donlon, E.A., Forti, A.A., Silva, V.P., Bruno, B.A., Carroll, M.K.: Synthesis and characterization of copper-nanoparticle-containing silica aerogel prepared via rapid supercritical extraction for applications in three-way catalysis. MRS Advances. **2**(57), 3485–3490 (2017)
28. Posada, L.F., Carroll, M.K., Anderson, A.M., Bruno, B.A.: Inclusion of ceria in alumina- and silica-based aerogels for catalytic applications. J. Supercrit. Fluids. **152**, 104536 (2019)
29. Harris, D.C.: Quantitative Chemical Analysis, 9th edn. W. H. Freeman, New York (2016)
30. Reichenauer, G., Scherer, G.W.: Nitrogen sorption in aerogels. J. Non-Cryst. Solids. **285**(1–3), 167–174 (2001)
31. Hirakawa, T., Shimokawa, Y., Tokuzumi, W., Sato, T., Tsushida, M., Yoshida, H., Hinokuma, S., Ohyama, J., Machida, M.: Multicomponent spinel oxide solid solutions: a possible alternative to platinum group metal three-way catalysts. ACS Catal. **9**(12), 11763–11773 (2019)